High-Dimensional Chaotic Dynamics of an External Cavity Semiconductor Laser

I. Fischer, O. Hess, W. Elsäßer, and E. Göbel

Fachbereich Physik and Material Science Center, Philipps-Universität Marburg, Renthof 5, D-35032 Marburg, Germany
(Received 24 January 1994)

We report experimental realization of high-dimensional chaos in a semiconductor laser with delayed feedback from a T-shaped cavity. We study the transition phenomena from regular to high-dimensional chaotic behavior and analyze the time series quantitatively. Correlation dimensions up to $C_2 \simeq 7$ are determined reliably from experimental data by a combination of a singular value analysis and a Grassberger-Procaccia algorithm. Modeling the dynamical behavior using semiclassical delay rate equations provides a basic understanding of the observed delay-induced instabilities.

During the last 15 years the investigation of nonlinear dynamics in optical systems has proven to be extremely fruitful for the understanding of nonlinear systems in general. Many experimental systems and theoretical models in optics have been of fundamental importance for the achievements in this area. In the past, the main interest has been the investigation and understanding of systems with only a few degrees of freedom (≤ 3). In particular, much progress has been made concerning possible bifurcations and phenomena at the transition from regular behavior to low-dimensional chaos. Investigations of high-dimensional chaos, on the other hand, have been mainly limited to numerical simulations; experiments have always had the problem of reliable and quantitative data analysis. Consequently, there has been a lack of configurations up to now that allow well-defined access to all, experiment, data analysis, and modeling.

A laser system with many interacting degrees of freedom can conveniently be realized by time-delayed feedback. The nonlinear dynamical behavior of a system with time-delayed feedback was first investigated theoretically by Ikeda *et al.* in the late 1970's [1,2] modeling a passive nonlinear ring resonator, externally pumped by a laser. Their investigations based on numerical modeling were later generalized to a simple delay equation applicable to a whole class of delay systems [3]. The *Ikeda scenario* turned out to be a paradigm for the dynamical behavior of delayed feedback systems. Two interesting phenomena predicted by the Ikeda scenario are a period doubling route to chaos and multistability. In experiments on passive systems, these phenomena related with low-dimensional dynamics have been verified [4,5]. Simulations also showed the occurrence of attractor fusion and high-dimensional chaos proving the high dimensionality of delayed feedback systems [3].

We have designed a setup with which a whole class of delay scenarios can be realized by simple modifications of its configuration. In particular, we have studied experimentally the influence of coherent optical feedback from a Michelson interferometerlike T-shaped cavity on the intensity dynamics of a semiconductor laser. This allowed us for the first time to realize experimentally and

to characterize reliably high-dimensional temporal chaos. We observe the coexistence of various different attractors, chaotic itinerancy among the unstable attractor ruins, and high-dimensional chaos. To corroborate the high dimensionality of the dynamical behavior, we combined a singular value analysis (SVA) with a usual modified Grassberger-Procaccia analysis for the determination of correlation dimensions. Moreover, by providing phase information numerical integration of model equations gives additional insight into the basic physical mechanism involved in the instabilities.

Our experimental setup is depicted in Fig. 1(a). We have employed a dc-driven GaAs/GaAlAs bulk semiconductor laser (Hitachi HLP1400). The facet facing the external cavity is antireflection (AR) coated with a residual reflectivity of $R_r \sim 10^{-4}$ in order to get a better coupling to the cavity and to avoid the coherence collapse. The injection current was held below the threshold of the soli-
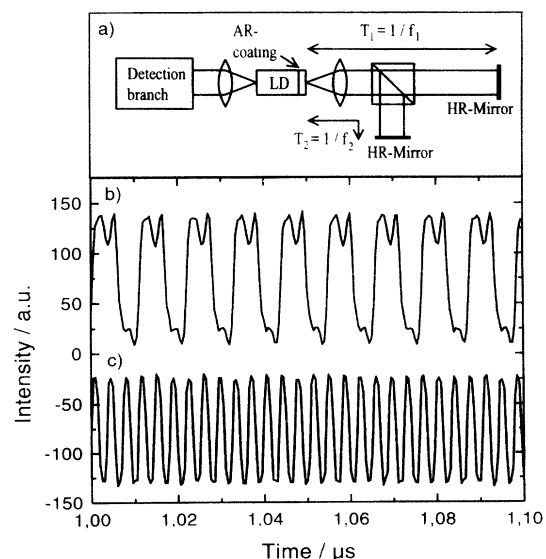

FIG. 1. (a) Experimental setup: Semiconductor laser (LD) coupled to a T-shaped external cavity. Periodic time series: (b) fundamental state with characteristic rectangular modulation; (c) third harmonic state.

tary laser diode. The T–shaped cavity consists of the uncoated facet of the laser diode (LD) and two external high reflecting gold mirrors ($R \approx 98\%$). A beam splitter divides the light intensity equally to the two cavity arms with the external mirrors. The lengths of the two arms are varied in the range 30 cm $\leq l_{1,2} \leq$ 1.5 m corresponding to round trip frequencies of 500 MHz $\geq$ $1/T_{1,2} = c/2\, l_{1,2} \geq$ 100 MHz.

The emission of the laser is detected and analyzed in the following manner. The time-integrated output power of the semiconductor laser is measured with a slow Si pin photodiode. The fast intensity fluctuations are detected by a fast Si avalanche photodiode. Its electrical output signal is amplified and then analyzed in the time and frequency domain using a fast digital oscilloscope (bandwidth 1 GHz) and a rf-spectrum analyzer. In addition, the optical spectrum can be measured with low resolution by an optical spectrum analyzer ($\Delta\lambda \approx 0.1$ nm) and with high resolution by a plane Fabry-Pérot interferometer ($\Delta\nu \approx 100$ MHz) [6].

We have designed this special cavity configuration in order to realize a class of systems, which show delay induced instabilities, that can be chosen by simple modifications of the configuration. In this Letter we will concentrate on the investigation of the T-resonator system with one of the delay times (T_1) being twice as long as the other one (T_2). As we will demonstrate in the following, an Ikeda-scenario–related behavior is observed in this case. Although the Ikeda scenario has originally been derived for passive single delayed feedback systems, our experiment shows a close relation to the Ikeda scenario with respect to the occurring dynamical states. In this context the additional delayed feedback with T_1 is to be regarded simply as a means for increasing the nonlinearity of the feedback function of T_2.

General features of the Ikeda scenario can be summarized as follows. Depending on the feedback strength μ, multistability of different states occurs, whose modulation period is given roughly by $T_n = 2\tau/(2n + 1)$, $n = 0, 1, 2, \dots$. For $n = 0$ the modulation is squarelike, and in the following called the fundamental state. With respect to their modulation frequency, the other states are called third harmonic state, fifth harmonic state, etc. For increasing μ each of the periodic states evolves on an individual branch to chaotic states, and finally a global chaotic attractor occurs by fusion of all individual chaotic attractors. The transition to chaos occurs on the fundamental branch via a period doubling cascade, and on the higher harmonic branches via splitting in coexisting isomer states, which are characterized by different peak modulation patterns superimposed on the original oscillations. They can be periodic as well as chaotic.

In addition to Ikeda's findings, we find switching between various states despite fixed experimental parameters. The lifetimes of the states which can be fixed points, periodic as well as chaotic states, range from ms up to some seconds. The fixed point corresponds to a

time independent constant light intensity. The periodic states can be categorized into different groups according to their dominant frequency in the power spectrum and related to the different branches in the Ikeda scenario. One group is defined by states with a dominant modulation frequency, which is nearly half of the compound cavity frequency, where the cavity frequency is given by the smallest common multiple of the individual round trip frequencies. Drawing an analogy to the Ikeda scenario, this modulation frequency is labeled as the fundamental frequency and the corresponding state as the fundamental state. The laser output of this state shows the characteristic rectangular modulation. The other groups of periodic states exhibit odd harmonics of the fundamental frequency as the dominant modulation frequencies. In our experiment, the seventh harmonic has been the highest state to be observed. The different groups include states with constant amplitude, as well as isomer states, characterized by different superimposed amplitude modulations. Two examples of periodic time series are shown in Figs. 1(b) and 1(c). The time series in Fig. 1(b) depicts an intensity modulation with the fundamental frequency; Fig. 1(c) shows one with the third harmonic. Each of these different groups can transform into individual chaotic states, and finally the global chaotic attractor can be observed.

In the regime of attractor fusion we have observed chaotic itinerancy—the phenomenon that a dynamical system switches among different unstable local chaotic orbits on a time scale, long compared to the dynamics on each attractor ruin. This effect, as it has been found in different computer models describing multimode lasers [7], coupled laser systems [8,9], coupled nonlinear oscillators [10,11], and neural networks [12], seems to be a general phenomenon in systems with many interacting degrees of freedom. A related effect has been found in a spatially extended Ikeda-like model [13]. Application of chaotic itinerancy as a method for adaptive search has been proposed by Davis for a passive optical system [14]. To our knowledge experimental verification has only been realized in a transverse multimode cavity with a photorefractive crystal [15].

One example of the experimental time series that verifies the switching among local chaotic attractor ruins is depicted in Fig. 2(a). It shows a transition from the local chaotic attractor ruin of the fundamental to the ruin of a third harmonic state. The transition itself is quite fast, taking place on a time scale comparable to only a few oscillation periods. The time which the system spends on a single attractor ruin varies in between 10 and 1000 periods. The depicted time series corresponds to the state at the final attractor fusion which leads to the global chaotic attractor. A time series attributed to the global chaotic attractor is shown in Fig. 2(b). Different regions can be distinguished which can be associated with the former local attractors. Regions with a modulation corresponding to the fundamental, the third, and the fifth
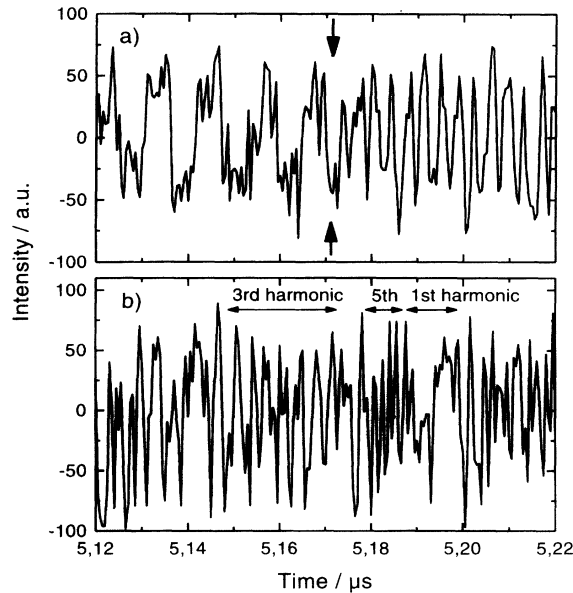
FIG. 2. Chaotic time series: (a) transition in time series showing chaotic itinerancy among chaotic fundamental and third harmonic states; (b) dynamics on the global chaotic attractor.
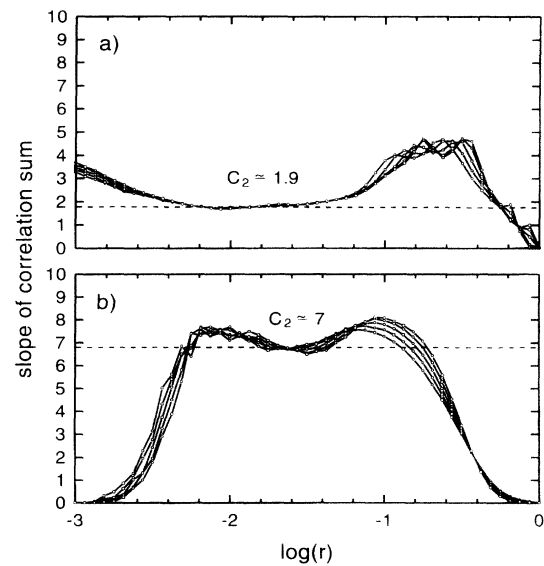

FIG. 3. Correlation dimension analysis. Slope of correlation sum versus radii obtained by the method described in the text: (a) low-dimensional local chaotic attractor; (b) high-dimensional local chaotic attractor.

harmonic frequency are particularly designated in the figure.

To characterize the chaotic time series and to verify our interpretation, we have performed correlation dimension calculations. They prove that the time series have dimensions which are distinctively larger than 3. The usual Grassberger-Procaccia analysis (GPA) [16] performed on the delay-embedded phase space requires a huge amount of data of high precision to achieve dimensions larger than 3. Our time series were experimentally restricted to 32 768 points. The noise level is estimated to be around 1%. This demands an improved method to reliably calculate higher dimensions. We expanded the usual GPA by applying a singular value decomposition [17] on the time series and reconstructing the phase space by a multichannel delay embedding of the principal components thus obtained [18,19]. This method has the advantage that both noise reduction as well as much better embedding of the phase space can be achieved, allowing the calculation of higher correlation dimensions. Clear scaling regions can be achieved yielding dimensions up to $C_2 \sim 7$ from experimental data [20]. In Fig. 3 results of the data analysis are shown, applied to two states on the fundamental branch. The diagrams show the slope of the correlation sum versus the radii of the spheres used for the counting in the GPA. Figure 3(a) shows the analysis of a low-dimensional chaotic state with chaotic period 4 according to the inverse period doubling cascade. A clear scaling region can be recognized between $\ln(r) = -2.2$ and $\ln(r) = -1.4$, yielding a dimension $C_2 \simeq 1.9$. Figure 3(b) depicts the result of our analysis applied to a higher-

dimensional local chaotic attractor with chaotic period 1 which is quite close to the attractor fusion. From the diagram one obtains the dimension $C_2 \simeq 7$. The analysis of the global chaotic attractor, however, no longer yields any clear scaling region, due to its even higher dimensionality. To check our analysis versus colored noise, we have performed the same analysis with surrogate time series [21]. In contrast to the original time series, no scaling regions can be seen in the case of the surrogates. But even for the global chaotic attractor, the analysis shows significantly different results for original and surrogate time series, an indication for the deterministic nature of the dynamical phenomena.

To give further evidence that the behavior of our system is determined by the delayed feedback, we have performed numerical modeling. It is based on the phenomenological rate equations for the optical field $\mathcal{E}$ and the inversion N of the semiconductor laser with time-delayed feedback as introduced by Lang and Kobayashi [22]. We have modified these equations by adding a second coherent feedback term to account for the second cavity arm:

$$\dot{\mathcal{E}}(t) = \left\{ i\omega(N(t)) + \frac{1}{2}[G(N(t)) - \Gamma] \right\} \cdot \mathcal{E}(t)$$
$$+ \kappa \cdot \mathcal{E}(t - T_1) + \kappa \cdot \mathcal{E}(t - T_2),$$

$$\dot{N}(t) = J - \gamma_{\parallel} N(t) - G(N(t)) \cdot |\mathcal{E}(t)|^2, \qquad (1)$$

where $G(N) = \Gamma + G_N(N - N_{tr})$ is the linearized gain function, $\omega(N) = \omega_0 - \alpha G_N(N - N_{tr})/2$ the lasing frequency, $\alpha = -2\omega_N/G_N$ the linewidth enhancement factor, N_{tr} the threshold inversion, Γ the inverse photon lifetime, $\gamma_{\parallel}$ the inverse electron lifetime, and J the pumping. Typical parameter values for this laser type have been used in the calculations [19]. On the basis of this model we can reproduce the experimental behavior

qualitatively. In addition, this numerical modeling allows us to get insight into the phase dynamics, which remains concealed in the experiment. This provides a deeper understanding of the physical mechanism, as illustrated in Fig. 4, where two examples of time series obtained by these simulations are shown. Note the striking similarity to the experimental time series shown in Fig. 1. In Fig. 4(a) the fundamental state is depicted. The different curves show the time dependence of the laser intensity I and Φ_1 and Φ_2, defined by the difference between the phase of the respective delayed optical field and the field inside the laser. The time dependence of the intensity is sensitively dependent on the delay phase differences Φ_1 of the longer cavity arm and Φ_2 of the shorter cavity arm. As can be seen in the figure, Φ_2 shows a strong modulation in the range $-\pi \leq \Phi_2 \leq 0$. The other delay phase difference is only marginally modulated around $\Phi_1 \sim 0$. The modulation of Φ_2 is transformed to an amplitude modulation, due to the delayed feedback. An additional coupling of amplitude and phase of the laser field is mediated by the α parameter. Shortly before each phase change there is a small overshoot to the respective opposite direction. This can be attributed to the pass of the phase over the maximum of the resonance curve of the compound cavity, which shifts with the laser intensity. The combination of these effects leads to the characteristic rectangular modulation. In Fig. 4(b) the third harmonic state is depicted. As can be seen from the plot of Φ_1 and Φ_2, the same mechanism applies as for the fundamental state. Furthermore, in the fifth harmonic state, period doubling, isomers, and chaotic states can be reproduced by the calculations. Thus, experiment and modeling confirm and complement each other with respect

to characterization and understanding of the dynamical behavior.

In conclusion, we have studied the transition from regular to high-dimensional chaos in a delayed feedback semiconductor laser system showing attractor merging and chaotic itinerancy. Various dynamical states are identified and quantitatively characterized by correlation dimensions up to $C_2 \sim 7$. Numerical modeling based on delay rate equations shows that the delay phases govern the observed instability. Presenting for the first time an experimental system which allows thorough analysis of the transition from regular behavior to high-dimensional chaos, we propose our model system as an ideal candidate for studying the dynamics in nonlinear systems with many degrees of freedom.

[1] K. Ikeda, Opt. Commun. **30**, 257 (1979).
[2] K. Ikeda, H. Daido, and O. Akimoto, Phys. Rev. Lett. **45**, 709 (1980).
[3] K. Ikeda and K. Matsumoto, Physica (Amsterdam) **29D**, 222 (1987).
[4] H. M. Gibbs, F. A. Hopf, D. L. Kaplan, and R. L. Shoemaker, Phys. Rev. Lett. **46**, 474 (1981).
[5] H. Nakatsuka, S. Asaka, H. Itoh, K. Ikeda, and M. Matsuoka, Phys. Rev. Lett. **50**, 109 (1983).
[6] The emission of the external cavity semiconductor laser shows several longitudinal modes of the external cavity.
[7] K. Ikeda, K. Otsuka, and K. Matsumoto, Prog. Theor. Phys. Suppl. **99**, 295 (1989).
[8] K. Otsuka, Phys. Rev. Lett. **65**, 329 (1990).
[9] K. Otsuka, Phys. Rev. A **43**, 618 (1991).
[10] K. Kaneko, Physica (Amsterdam) **54D**, 5 (1991).
[11] K. Kaneko, Physica (Amsterdam) **68D**, 299 (1993).
[12] I. Tsuda, *Neurocomputers and Attention: Neurobiology, Synchronization and Chaos* (Manchester University Press, Manchester, U.K., 1991).
[13] M. Sauer, J. Leonardy, and F. Kaiser (to be published).
[14] P. Davis, Jpn. J. Appl. Phys. **29**, 1238 (1990).
[15] F. T. Arecchi, G. Giacomelli, P. L. Ramazza, and S. Residori, Phys. Rev. Lett. **65**, 2531 (1990).
[16] P. Grassberger and I. Procaccia, Phys. Rev. Lett. **50**, 346 (1983).
[17] R. Vautard, P. Yiou, and M. Ghil, Physica (Amsterdam) **58D**, 95 (1992).
[18] K. Fraedrich and R. Wang, Physica (Amsterdam) **65D**, 373 (1993).
[19] I. Fischer, O. Hess, W. Elsäßer, and E. Göbel (to be published).
[20] The method was extensively tested with different parameter sets, which confirmed the convergence of the method.
[21] J. Theiler, S. Eubank, A. Longtin, B. Galdrikian, and J. D. Farmer, Physica (Amsterdam) **58D**, 77 (1992).
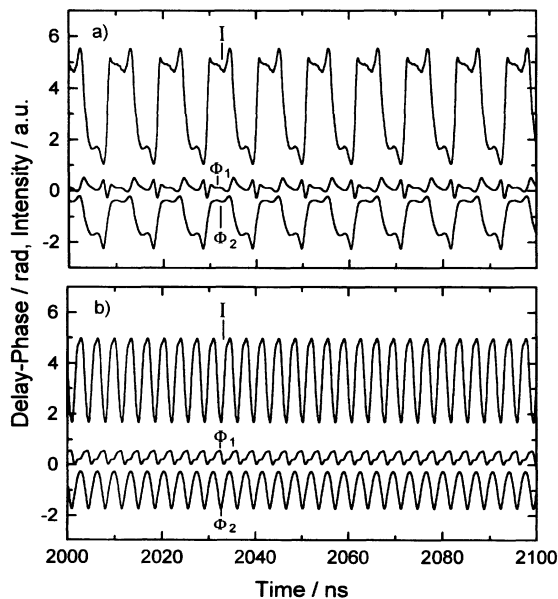[22] R. Lang and K. Kobayashi, IEEE J.Quantum Electron. **16**, 347 (1980).

FIG. 4. Calculated time series of laser intensity and delay phases: (a) fundamental state with characteristic rectangular modulation; (b) third harmonic state.